Korean Membrane Journal
Vol. 6, No. 1 December, 2004, 61-69

The Observation of Nucleation & Growth during Water Vapor Induced Phase Inversion of Chlorinated Poly(vinyl chloride) Solution using SALS

Jae Young Jang, Young Moo Lee, and Jong Seok Kang*†

School of Chemical Engineering, College of Engineering, Hanyang University, Seoul 133-791, Korea
*Department of Technology Information Analysis, Korea Institute of Science and Technology Information (KISTI), Seoul 130-742, Korea
(Received November 10, 2004, Accepted November 26, 2004)

Abstract: Small angle light scattering (SALS) and field emission scanning electron microscope (FE-SEM) have been used to investigate the effects of alcohol on phase separation of chlorinated poly(vinyl chloride) (CPVC)/tetrahydrofuran (THF)/alcohol (9/61/30 wt%) solution during water vapor induced phase separation. A typical scattering pattern of nucleation & growth (NG) was observed for all casting solutions of CPVC/THF/alcohol. In the case of the phase separation of CPVC dope solution containing 30 wt% ethanol or n-propanol, the demixing with NG was observed to be heterogeneous. Meanwhile, the phase separation of CPVC dope solution with 30 wt% n-butanol was found to be predominantly homogeneous NG. Although the different phase separation behavior of NG was observed with types of alcohol additives, the resultant surface morphology had no remarkable differences. That is, even though the NG process by water vapor is either homogeneous or heterogeneous, this difference does not play a main role on the final surface morphology. However, it was estimated from the result of hydraulic flux that the phase separation by homogeneous NG provided the membrane geometry with lower resistance in comparison with that by heterogeneous one.

Keywords: *nucleation & growth, chlorinated poly(vinyl chloride) (CPVC), alcohol additive, small angle light scattering (SALS), hydraulic flux*

1. Introduction

Processes of phase separation of polymeric solutions by nonsolvent addition are a usual method for obtaining films with porous structure, especially in the membrane field[1]. The separation of homogeneous mixture into two phases can proceed through two main ways, spinodal decomposition (SD) and nucleation & growth (NG)[2,3]. The selection of the mechanism will depend on the thermodynamic balance between the two components and is mainly driven by the quenching depth and the composition[4]. Also, the mechanism of phase separation is controlled by the depth of penetration into the unstable region. When the phase separation process occurs between binodal and spinodal (metastable region), this process is called nucleation & growth (NG)[2,3]. The solution is stable to small fluctuations but undergoes phase separation for large concentration fluctuations. A dispersed phase consisting of droplets of a polymer poor solution is formed in a concentrated matrix. The composition inside the nuclei does not change with time, and only the size of the droplets increases with time. The molecules that feed the new phase follow ordinary transport phenomena by downhill diffusion with a positive diffusion coefficient. Meanwhile, if the demixing path penetrates below binodal boundary (unstable region), spinodal decomposition mechanism (SD) is favored. All concentration fluctuations result in a decrease of free energy and lead to a spontaneous phase separation.

Analysis of the time progression and the angular distribution of scattered light made it possible to

†Author for all correspondences
(e-mail : kangjs@kisti.re.kr)

establish the phase separation mechanism of NG or SD. In both cases, since the system will be transformed from a homogeneous mixture with singe refractive index to a mixture with two different refractive indexes, small angle light scattering (SALS) is the obvious and the most simple tool to study such phase separation in the type of systems under consideration here[5-7,16]. The availability of SALS depends on the length scale window of interest. SALS (He-Ne laser) can provide an adequate spatial resolution for studying the phase separation, typically covering the fluctuation of a few micron-scale[8]. In this paper, SALS technique has been widely used to investigate the phase separation mechanism for polymer systems[9,14,23]. Here, we applied SALS technique to confirm the phase separation mechanism for the chlorinated poly(vinyl chloride) (CPVC)/THF/alcohol dope solution, in a concentration range normally considered for casting solutions, nucleation & growth might be the predominant event during water vapor quenching of the dope solution.

This paper presents the results of the scattering patterns with time evolution and the surface morphology by field emission scanning electron microscopy to investigate the effects of alcohols such as ethanol, n-propanol and n-butanol on phase separation of CPVC/THF/alcohol solution during water vapor induced phase separation. Analysis of scattering and the angular distribution of scattered light intensity were carried out by monitoring the progression of scattering pattern with time evolution. Also, the phase inversion rate of nonsolvent induced phase separation (NIPS) shows the extremely fast kinetics (frequently less than a second). Therefore, it is almost impossible practically to observe this process within a reasonable time scale; the preceding rate of phase inversion was allowed to be very slow by the vapor of the nonsolvent instead of the liquid media, resulting in simply monitoring the complete demixing process in a single experiment. Also, the surface morphology and the hydraulic flux were observed to investigate the effects of alcohol on the geometry for the quenched polymer solution.

2. Experimental Section

2.1. Materials and Dope Solutions

A chlorinated poly(vinyl chloride) (CPVC, Nippon Carbide Ind. Co. Inc., Tokyo, Japan) with a chlorine content of about 63-68% was used as a base material in this study. Tetrahydrofuran (THF, Aldrich Chemical Co., Milwaukee, WI, U.S.A.) and alcohols (ethanol, n-propanol and n-butanol (Junsei Co., Tokyo, Japan)) were used as solvent and nonsolvent additives, respectively. CPVC was dried under vacuum at 30°C for 12 hrs in order to minimize the presence of water in the polymer prior to the preparation of the solution. THF and alcohols were used as received without further purification.

CPVC dope solutions were prepared by dissolving CPVC in the co-solvent system. The composition of co-solvent was THF:alcohol = 70:30 wt%. Polymer dope solutions were prepared by increasing the number of carbon of primary alcohol while the concentration of CPVC in the solution was maintained to be 9 wt%.

2.2. Measurement

The setup of small angle light scattering (SALS) apparatus was described in detail elsewhere[10], and only a brief account was given here. The scattering intensity, I, is measured as a function of the magnitude, q, of the scattering vector, denoted by $q = [4\pi \sin(\theta/2)]/\lambda]$, θ is the scattering angle of the intensity at maximum, and λ is the wavelength of the light (He-Ne 632.8 nm, 10 mW), respectively. As shown in Figure 1, a collimated laser beam impinges into sample, which is located in the rectangular glass chamber ($30\times30\times25$ cm) connected with the humidity controller (JEIO Tech. Model Sk-G001, Seoul, Korea). Both the transmitted and scattered light were projected on the opaque screen at the upper side of the rectangular glass chamber in whose focal plane a beam stop blocked the directly incident beam and the images of scattered light were recorded and digitized by the CCD (NTC/CCD-512-TK, Roper Scientific, Trenton, NJ, U.S.A.) with ST-133 controller. To obtain the scattered light intensity, $I(q)$,

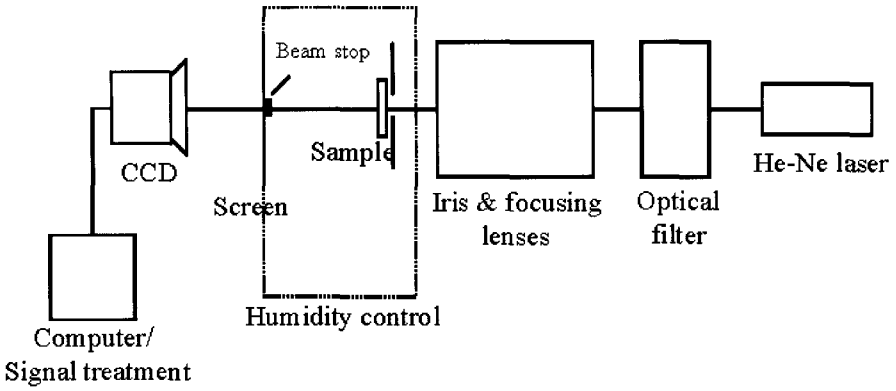

Fig. 1. Schematic of small angle light scattering apparatus.

as a function of time, the CCD output (512×512 pixels) was averaged over rings of pixels centered about the optical axis of the apparatus, which corresponded to the same magnitude, q, of the scattering vector. This setup allowed us to measure $I(q)$ over scattering vectors in the range of 0.398 $\mu m^{-1} < q < 3.72\ \mu m^{-1}$, corresponding to angles from 2.3° to 21.6°. The data from all angles can be recorded at a rate of 2 msec/scan. In a typical experiment, the scattered light intensities at different angles were recorded in real time for up to several minutes to document the time evolution of light intensities.

The SALS experiments were conducted by quenching the polymer solutions in water vapor from the one-phase region to the two-phase region at a given concentration. Scattering cells prepared by casting a thin film (50 μm) of dope solution on microscope slide were located on circular aperture and were exposed to the water vapor of RH53% (±3%) at 26°C in a glass chamber. During the water vapor quenching, scattered light intensities and patterns were monitored as an elapsed time.

The surface morphologies of the quenched films after SALS experiment were also determined using field emission scanning electron microscope (FE-SEM, JEOL-6340F, Kyoto, Japan) at an accelerating voltage of 15kV. Scattering cell was immersed in water to extract the residual solvent (THF/alcohol) and to solidify the resultant structure of film and then dried in vacuum at 30°C for 1 day. Dried specimen was fractured under cryogenic condition using liquid nitrogen and coated with gold to take the FE-SEM photographs.

A dead-end stirred cell filtration system[11-13] was used to measure the flux of deionized water through the prepared specimens. This apparatus consisted of a 50 mL filtration unit (Model 8050, Amicon Corp., W. R. Grace Corp., Beverly, MA, U.S.A.), a 4000 mL feed reservoir, a permeate collection reservoir, a pressure gauge and an electronic balance connected with a computer. The effective membrane area was 13.4 cm^2. All filtration experiments were carried out at a constant transmembrane pressure (TMP) of 0.05 MPa and a system temperature of 25±1°C. All the membranes were initially immersed into isopropylalcohol/H_2O (20/80 w/w%) mixture for 10 min before test. The weight of permeate was measured every 30 seconds with an electronic balance and then automatically recorded in an on-line computer.

3. Results and Discussion

3.1. Scattering During Spinodal Decomposition and Nucleation & Growth

As far as liquid-liquid demixing of polymer solution is considered, two different mechanisms have to be considered: nucleation & growth (NG) and spinodal decomposition (SD). NG is the expected mechanism when a system leaves the thermodynamically stable condition and slowly enters the metastable region of phase diagram, between the binodal and the spinodal

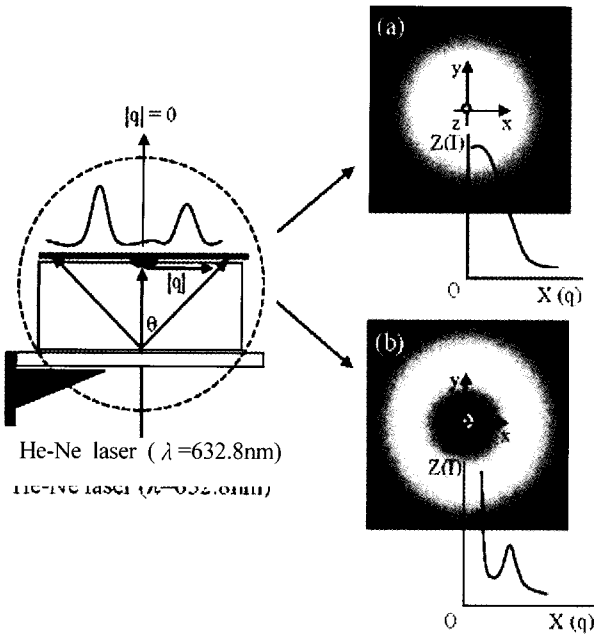

Fig. 2. Typical scattering patterns of phase separation processes: (a) nucleation & growth, (b) spinodal decomposition.

line. Dispersed nuclei are formed and become stable if the activation energy for nuclei formation is higher than the surface free energy. NG is usually a slow process, and a large number of polymeric systems have been reported in the literature in which phase separation follows the NG[14-17]. For the investigation of NG, time resolvable light scattering measurements with angle dependence have been especially useful. As illustrated in Figure 2, when the NG mechanism predominates, a monotonic decrease of scattered light intensity with angle is normally observed[18]. At a fixed angle, the increase of scattered light intensity can be fitted to a power law[19]. However, in the case of phase separation accompanied by any chemical reaction, these power law equations are not considered.

Meanwhile, light passing through the SD structure with high periodicity is diffracted, forming a scattering halo. The halo formation can be better understood in the following way. During spinodal decomposition, each concentration fluctuation with a wavenumber q, indicating the correlation length in a network of entangled polymers (or the size of aggregates in solution), contributes to diffraction at an angle θ. In an early stage described by the Cahn-Hilliard linearised theory[20-22], some fluctuations with a wavenumber q_m were predominant and contributed to a maximum scattered light intensity at an angle θ_m, giving rise to the observed halo. Also, the evolution of the structural factor with time was characterized by an exponential growth with a fixed maximum located around q_m.

In both cases, since the system will be transformed from a homogeneous mixture with a single refractive index to a mixture with two distinct phases (with two different refractive indexes), small angle light scattering (SALS) is the obvious, most simple tool to study such phase separations in the type of NG or SD.

3.2. The Observation of Time-Resolved Small Angle Light Scattering During NG

The evolution of light scattering patterns with time during quenching with water vapor of RH53% were observed for transparent CPVC solutions (CPVC/THF/ROH = 9/61/30 wt%), where the alcohols (ethanol, n-propanol and n-butanol) were used as the nonsolvent additive within dope solution, respectively. All scattering pictures were presented as detected by the CCD camera without subtracting a background image, where the time indicated the elapsed time of each experiment. The run was sufficiently maintained for several minutes in order to observe the full stage behavior of NG as clear as possible. The existence of the fractal regime at very small scattering vectors ($q \ll R^{-1}$) reveals the existence of structures on length scales larger than R, where R is the size of the supermolecular structure; this can result from the presence of large aggregates or from entanglements in concentrated solutions. The fractal dimension at low q provides a measure of the supramolecular organization of the solution. In these cases, a concentration fluctuation of polymer solution may be visible at low q, indicating the correlation length (in a network of entangled polymers), or the size of aggregates in solution. As already described in experimental section, this setup allowed us to measure $I(q)$ over scattering vectors in the range of 0.398 μm^{-1} < q <3.72 μm^{-1}, showing the fluctuation of the supra-

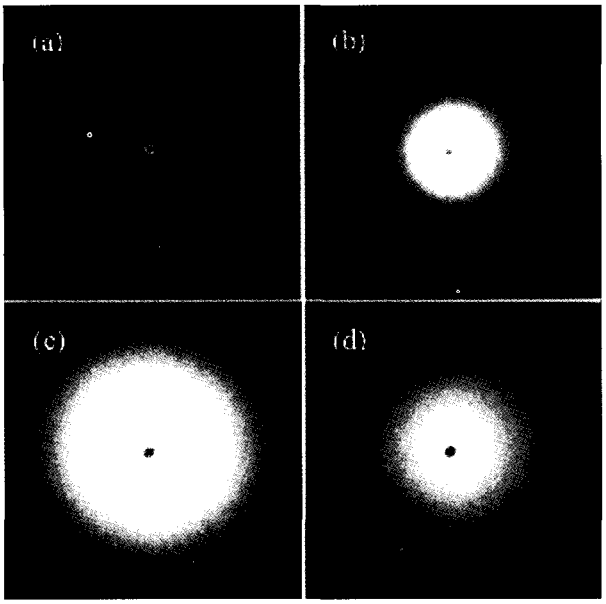

Fig. 3. Representative SALS patterns for proceeding phase separation of 9 wt% CPVC solution/81 wt% TFH/10 wt% n-butanol system under RH53% (±3%) at 26°C (a) 117.0 sec, (b) 120.0 sec, (c) 271.5 sec, and (d) 294.0 sec.

molecular organization of the solution within the several micron scale.

Representative light scattering patterns were shown in Figure 3. It was seen from Figure 3 that after ca. 120 sec water vapor exposure to water vapor, the corn-typed scattering pattern appeared in the detectable region; immediately the maximum intensity increased and became broader with time. Thereafter, as indicated in the late stage of the phase separation process, a scattering intensity finally became weak and decreased with time, and maintained a smaller corn-typed pattern. These characteristic SALS patterns showed a typical phase separation following NG.

Also, Figure 4 showed the light scattering patterns progressed as a function of time during SD. It could be observed from Figure 4 that the scattering maximum appeared within experimental time scale; immediately the maximum intensity increased and became broader with time. Thereafter, as indicated in the late stage of the phase separation process, a scattering intensity at the inner side of halo distinctively appeared during the very short time-interval and finally got closer to the first and then turned into a broader one of corn-typed patterns. Therefore, the difference between scattering pattern at the late stage of SD and NG was not clearly observed due to a similar SALS patterns, as compared in Figure 3(d) and Figure 4(d). Therefore, it could be considered that phase separation was interrupted by gelation, glass transition, or crystallization [23]. However, in early stage of phase separation, NG and SD from SALS pattern was relatively well distinguished, as shown in Figure 3 and 4.

3.3. Analysis of the SALS Patterns During NG

Figure 5 showed the intensity profiles of scattered light as a function of time monitored after consecutive time. As shown in Figure 5, for all casting solutions of CPVC/THF/alcohol, the intensity of the scattered light increased steadily with time. Also, the intensities continually increase without displaying maximum I value, as q values decrease. For spinodal decomposition

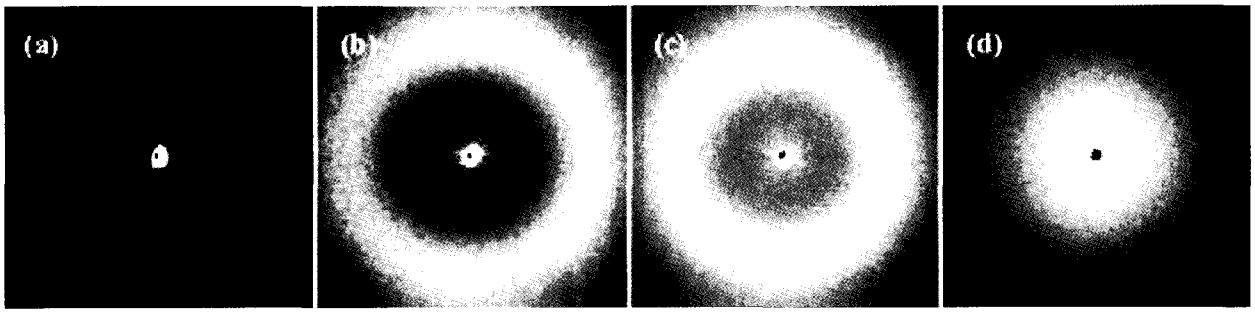

Fig. 4. The light scattering patterns progressed as a function of time during phase inversion process under water vapor of RH53% using Psf/NMP/n-butanol system. Typical SALS patterns of SD with time evolution[24]. (a) before phase separation, (b) the early stage of SD, (c) the intermediate stage of SD, and (d) the late stage of SD.

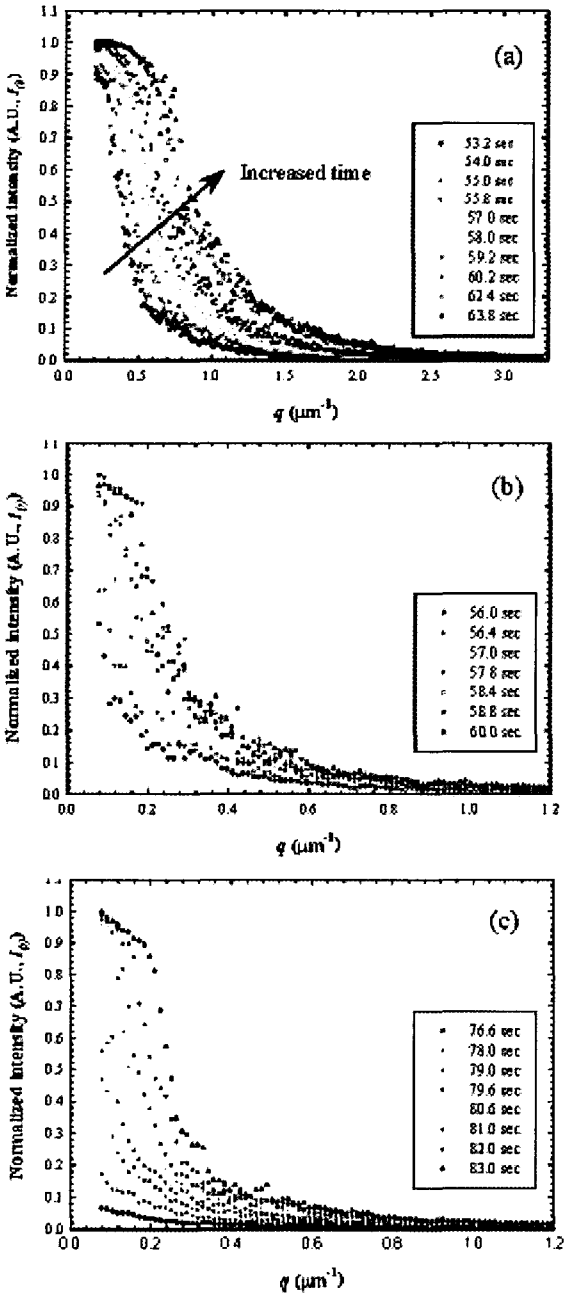

Fig. 5. Time evolution of the normalized scattering intensity profiles, $I_{(t)}/I_0$, during phase separation under RH53% at 26°C: (a), (b), and (c) are the result of CPVC solution with 30 wt% ethanol, n-propanol, and n-butyl alcohol, respectively.

system, scattered light intensities increase with time and show a scattering maximum growing with time, as shown in Figure 4. But, in this system, the intensity of the scattered light increases with time, but there is not

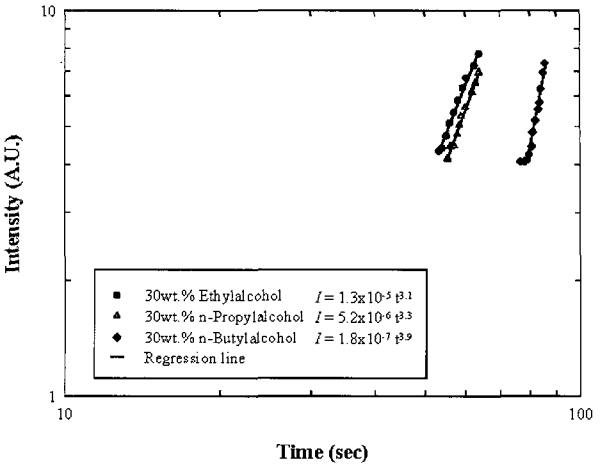

Fig. 6. Logarithmic plot of light scattering intensity as a function of time for CPVC solutions.

a sign of a maximum. The spinodal ring could not be observed. These results show reliable evidence that the phase separation mechanism of this system develops under nucleation & growth. The intensity of the scattered light is detected as a function of the scattering angle and time. As the solution became opaque with water vapor of RH 53%, the intensity of the scattered light decreases steadily with increasing angle. At a constant angle, it increased as a function of time by a power law reflecting the detail of the process.

Figure 6 shows double logarithmic plots of intensities as a function of time for CPVC/THF/alcohol (9/61/30 wt%). The time dependence of scattered light at constant angle follows the power law[19]:

$$I(\theta) = k(t-\tau)^n \qquad \text{(eq. 1)}$$

where K represents a growth constant, τ is the initial time (usually arbitrated as zero) and n is the time for phase separation, and n is the slope in a log-log plot during the NG process. Nuclei are by and large created at random time (heterogeneous NG) or simultaneously (homogenous NG) and grow subsequently. The NG process can be in two forms: homogeneous, wherein the spheres are produced in a simultaneous fashion and they grow in the same way; or heterogeneous, wherein the spheres are produced at various times, and they

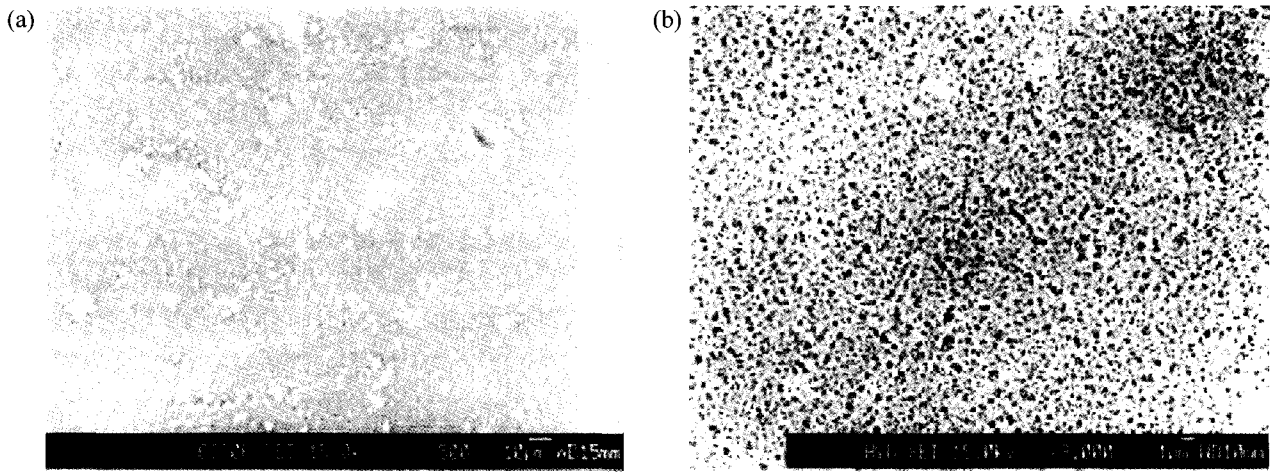

Fig. 7. Representative surface morphology prepared by CPVC dope solution with 30 wt% n-butanol. (a) and (b) are SEM photographs enlarged with ×500 and ×3,000, respectively.

vary diversely in sizes. Heterogeneous NG is indicated by values of n close to 3, while an n value of 4 is characteristic of homogeneous NG. The value for n can be obtained from the curve by plotting log (I) versus log ($t-\tau$). When a straight line with a slope close to 3 (n = 3) is generated from the plot, it insinuates a heterogeneous nucleation mechanism. On the other hand, homogeneous nucleation is suggested if the best fit is obtained with n = 4.

For CPVC/THF/ethanol and CPVC/THF/n-propanol system, the values of slope, n, were calculated to be 3.1 and 3.3, respectively. Also, K values for the former and latter are 1.3×10^{-5} and 5.2×10^{-6}, respectively. These results showed that both solutions stated above proceeded with a heterogeneous NG mechanism. Meanwhile, for CPVC/THF/n-butanol system, the values of slope, n, and K were calculated to be 3.1 and 1.8×10^{-7}, respectively. That is, the mechanism of phase separation for the dope solution containing 30 wt% n-butanol showed a homogenous NG. It is well known that homogeneous NG occurs at the slower process than heterogeneous NG does[14]. However, the effects of phase inversion with heterogeneous or homogeneous NG on the final structure of quenched film, as well as the surface morphology were not clearly reported. The hydraulic flux measurement of films quenched by water vapor reveals the effects of alcohol on the geometry of the final structure, which will be discussed in the following section.

3.4. Surface Morphology and Hydraulic Flux

Membranes produced by coagulating the polymer solution in a liquid nonsolvent media exhibited in general a more or less dense surface morphology, while the membranes made by water vapor induced phase separation showed a microporous surface morphology. Given that water acts in a similar way in vapor phase as it would be in the liquid phase, the membrane - through which separation of water vapor is induced - should demonstrate a similar morphology with the one coagulated by liquid water, since the thermodynamic state of all the other components stays the same. The difference in two instances, hence, does not seem to be originated from thermodynamic differences, but from the kinetic ones.

A representative surface morphology guided from CPVC/THF/n-butanol (9/61/30 wt%) was presented in Figure 7. Up to now the mechanism of the formation of surface morphology has not been completely understood. However, it has been reported that membranes with microporous surface can be fabricated by evaporating the polymer solution[26]. Since THF has higher volatility than n-BA in the used co-solvent, n-BA/THF ratio increases during the evaporation stage. Therefore,

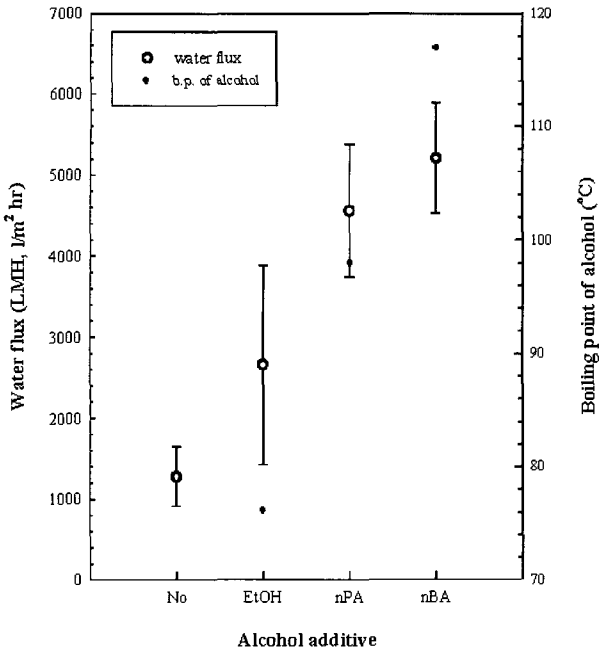

Fig. 8. The hydraulic flux of the CPVC film prepared by adding various alcohols to CPVC dope solution. Dotted circle and crosshair symbols denote the hydraulic fluxes of CPVC specimen and boiling point of alcohol, respectively.

it might be suspected that an increase of n-BA/THF ratio during solvent evaporation causes phase separation in casting solution and generates the pores on membrane surface. This suggestion made possible to explain the fact that the hydraulic flux increased with the boiling point of alcohol additive, as shown in Figure 8. However, in the present case, the membrane formation mechanism was not simply elucidated because of the combined process of solvent evaporation and water vapor adsorption.

Regardless of the type of alcohol additives, the surface morphology showed no observable differences. That is, even though the NG process by water vapor is either homogeneous or heterogeneous, this difference does not play a main role of the final surface morphology. However, their hydraulic flux showed a remarkable difference, as shown in Figure 8. It was estimated from the result of hydraulic flux that the phase separation by homogeneous NG provided the membrane geometry with lower resistance in comparison with that by heterogonous one.

4. Conclusions

The scattering patterns with time evolution and the surface morphology by field emission scanning electron microscopy were shown to investigate the effects of alcohol on phase separation of CPVC/THF/alcohol solution during water vapor induced phase separation. A typical scattering pattern of NG was observed for all casting solutions of CPVC/THF/alcohol. While the intensities continually decreased without displaying maximum I value, as q values increased, the intensity of the scattered light increased steadily with time. Also, in the case of the phase separation of CPVC dope solution containing 30 wt% ethanol or n-propanol, the demixing with NG was observed to be heterogeneous. Meanwhile, the phase separation of CPVC dope solution with 30 wt% n-butanol was predominantly investigated to be homogeneous NG. Although the different phase separation behavior of NG was observed with types of alcohol additive, the resultant surface morphology had no remarkable difference. However, their hydraulic flux showed remarkable differences due to the formation of the membrane geometry with lower resistance through the phase separation by homogeneous NG.

References

1. R. E. Kesting, *Synthetic polymeric membrane*, Wiley, NY (1985).
2. S. Komura and H. Fukukawa, *Dynamic ordering processes in condensed matter*, NY: Plenum Press (1983).
3. J. D. GuntonSan, M. Miguel, and P. S. Sahni, *Phase transition and critical phenomena*, vol.8. NY: Academic Press (1983).
4. M. Mulder, *Basic principles of membrane technology*, Kluwer Academic, Dordrecht (1991).
5. H. Matsuyama, M. Teramoto, R. Nakatani, and T. Maki, *J. Appl. Polym. Sci.*, **74**, 171 (1999).
6. K. V. Peinemann, J. F. Maggioni, and S. P. Nunes, *Polymer*, **39(15)**, 3411 (1998).

7. H. Matsutyama, M. Nishiguchi, and Y. Kitamura, *J. Appl. Polym. Sci.*, **77**, 776 (2000).
8. R. Viswanathan and D. W. M. Marr, *Langmuir*, **12**, 1084 (1996).
9. T. Inoue and T. Ougizawa, *J. Macromol. Sci. Chem.*, **A26**, 147 (1989).
10. L. Cipelletti and D. A. Weitz, *Rev. Sci. Instrum.*, **70**, 3214 (1999).
11. J. S. Kang, J. K. Shim, H. Huh, and Y. M. Lee, *Langmuir*, **17**, 4352 (2001).
12. J. K. Shim, Y. B. Lee, and Y. M. Lee, *J. Appl. Polym. Sci.*, **74**, 75 (1999).
13. J. K. Shim, H. S. Na, Y. M. Lee, H. Huh, and Y. C. Nho, *J. Membr. Sci.*, **190**, 215 (2001).
14. S. P. Nunes and T. Inoue, *J. Membr. Sci.*, **111**, 93 (1996).
15. J. Szydlowski and A. van Hook, *Macromolecules*, **31**, 3255 (1998).
16. E. Schuhmacher, V. Soldi, and A.T.N. Pires, *J. Membr. Sci.*, **184**, 187 (2001).
17. D. Pontoni, T. Narayanan, and A. R. Rennie, *Langmuir*, **18**, 56 (2002).
18. T. Hashimoto, *Current topics in polymer science*, Hanser, Munich, pp.199 (1987).
19. J. G. Wijmans, H. J. J. Rutten, and C. A. Smolders, *J. Polym. Sci., Polym. Phys. Ed.*, **23**, 1941 (1985).
20. J. W. Cahn and J. E. Hilliard, *J. Chem. Phy.*, **28**, 258 (1958).
21. J. W. Cahn and J. E. Hilliard, *J. Chem. Phy.*, **31**, 688 (1959).
22. J. W. Cahn, *J. Chem. Phy.*, **42**, 93 (1965).
23. P. D. Graham, A. J. Pervan, and A. J. McHugh, *Macromolecules*, **30**, 1651 (1997).
24. J. Maugey, T. van Nuland, and P. Navard, *Polymer*, **42**, 4353 (2001).
25. T. Kawai and Y. M. Lee, *Polyme*, **36**, 1631 (1997).